Luong Minh Chinh
Structure and Environment 2023, vol. 15, (2), pp. 63-72, Article number: el 006
https://doi.org/10.30540/sae-2023-006



Structure and Environment
ISSN 2081-1500
e-ISSN 2657-6902
https://content.sciendo.com/sae
https://sae.tu.kielce.pl

Kielce University of Technology

DOI: 10.30540/sae-2023-006

# USING SATELLITE IMAGES TO RETRIEVE THE RIVER TURBIDITY AND WATER FLOW VELOCITY FOR MONITORING THEIR INFLUENCES ON BRIDGE SUBSTRUCTURES

# WYKORZYSTANIE ZDJĘĆ SATELITARNYCH DO OKREŚLENIA MĘTNOŚCI WODY ORAZ PRĘDKOŚCI PRZEPŁYWU WODY RZEKI W CELU MONITOROWANIA ICH WPŁYWU NA PODPORY MOSTÓW

Luong Minh Chinh*
Thuyloi University Hanoi, Vietnam

**Abstract**

*Turbidity is an important indicator of water quality in rivers, lakes, and coastal areas. Research on turbidity issues in these areas is significant not only for the development and utilization of water resources for aquaculture, tourism, and other purposes but also for assessing the level of silt (sand) in the river, allowing sediment alluvial to build up a bank of the river, and monitoring the degree of water corrosion in the bridge substructure. This allows for the building of an effective maintenance and conservation program for the bridge in response to climate change.*

*Traditional methods have defined the turbidity of water in a local area, on a small scale. Interpolation errors of traditional methods for large areas may exceed over 20%. The use of remote sensing technology as Landsat-8 satellite images with a high geometric resolution of 30-meter multispectral channels allows us to estimate and distribute the water turbidity in a 30 × 30 m grid in detail.*

*Using multi-temporal Landsat-8 data in 2014 and 2015 for modeling water turbidity of Tien and Hau rivers and coastal areas in South Vietnam, the obtained mean absolute error is approximately 20%, the Root Mean Square Error (RMSE) does not exceed 10 NTU. The models have a high coefficient of efficiency ME, approximately 90% (ME = 0.862), and the correlation coefficient R stronger than 90%. This allows an overall assessment of changes in water flow velocity concerning the amount of sediment in the river.*

**Keywords:** turbidity monitoring, river banks erosion, bridge erosion, bridge maintenance, remote sensing

**Streszczenie**

*Mętność jest ważnym wskaźnikiem jakości wody w rzekach, jeziorach i obszarach przybrzeżnych. Badania nad tą kwestią są istotne nie tylko dla rozwoju i wykorzystania zasobów wodnych na potrzeby akwakultury, turystyki i innych celów, ale także dla oceny poziomu mułu (piasku) w rzece, pozwalającego osadom aluwialnym budowanie brzegu rzeki oraz monitorowanie stopnia korozji w podporach mostu. Umożliwi to opracowanie skutecznego programu konserwacji i utrzymania mostu w odpowiedzi na zmiany klimatyczne.*

*Tradycyjne metody pozwalają określić mętność wody w obszarze lokalnym, w małej skali. Błędy interpolacji tradycyjnych metod do dużych obszarów mogą przekraczać 20%. Zastosowanie technologii teledetekcji w postaci zdjęć satelitarnych Landsat-8 o wysokiej rozdzielczości geometrycznej 30-metrowych kanałów wielospektralnych pozwala na szczegółowe oszacowanie i rozmieszczenie zmętnienia wody w siatce 30 × 30 m.*

*Thuyloi University Hanoi Vietnam, e-mail: chinhlm@tlu.edu.vn

*Wykorzystując wieloczasowe dane Landsat-8 z lat 2014 i 2015 do modelowania zmętnienia wody rzek Tien i Hau oraz obszarów przybrzeżnych w południowym Wietnamie, uzyskany średni błąd bezwzględny wynosi około 20%, a średni błąd kwadratowy (RMSE) nie przekracza 10 NTU. Modele mają wysoki współczynnik efektywności ME, około 90% (ME = 0,862), a współczynnik korelacji R jest wyższy niż 90%, co stwarza możliwość dokonania ogólnej oceny zmian prędkości przepływu wody w odniesieniu do ilości osadów w rzece.*

**Słowa kluczowe:** monitoring mętności, erozja brzegów rzek, erozja mostów, konserwacja mostów, teledetekcja

## 1. INTRODUCTION

Riverbank erosion is one of the natural disasters causing many serious consequences in the floodplain of the Mekong Delta. The Tien River is one of the two main tributaries to the Mekong (along with the Hau River) as it flows into Vietnam. The Tien river across the Mekong Delta approximately 122.9 km [11]. The width of the Tien River changes many times, the thinnest point in An Long (Tam Nong) is about 450 m, the widest point in Long Khanh is 2.200 m, the average depth is about 10-15 m. The Tien River accounts for about 80% of the total water flow to the Mekong, average flow is 11500 $m^3/s$, maximum is 41504 $m^3/s$, smallest is about 2000 $m^3/s$, there are many curved and torsional sections, so very strong erosional activity and sedimentation take place [11, 12].

There are several large bridges across the Tien River: My Thuan Bridge (2000) (Figure 1), Cao Lanh Bridge (2018), Rach Mieu Bridge (2002), My Thuan Bridge 2 (under construction), while across the Hau River there are: Can Tho Bridge (2011), Co Chien Bridge (2018), Vam Cong Bridge (2018). These are cable-stayed bridges with large spans over 270 m, so all the impacts of the surrounding environmental factors on these structures are of significant importance, especially the impact of the flow velocity [13].

*Figure 1. The location of the My Thuan Bridge on the Tien River in Vinh Long Province*

The study of changes in the Tien and Hau riverbed, especially erosional situation to identify causes as a scientific basis to propose solutions to stabilize river banks, ensure structural diagrams of bridges (My Thuan Bridge), respond to climate change, and minimizing the damaging impact to the bridge is essential.

*Figure 2. Riverbank erosion of the Tien River, near to the My Thuan Bridge*

Traditional methods have defined the turbidity of water in a local area, on a small scale. Interpolation errors of traditional methods for large areas may exceed over 20%. Remote sensing technology as Landsat-8 satellite images with a high geometric resolution of 30-meter multispectral channels allows us to distribute the water turbidity in a 30 × 30 m grid in detail.

Remote sensing has been used around the world for several decades, started in the 1970s and 1980s when Landsat and Spot images appeared on the market. Since the beginning of the 21st century, many countries have been using remote sensing technology to monitor the quality of surface waters, not just those with their own satellites [2, 4, 5, 9]. High spatial resolution satellite images such as Worldview-2 (less than 0.5 m accuracy for the panchromatic – PAN image and 2.0 m for the multi-spectral image) were used to monitor coastal and continental water quality [4, 10, 15]. In Vietnam, the National Department of Remote Sensing, started using remote sensing technology to monitor surface water quality in 2010.

By utilizing multi-temporal Landsat-8 data from 2014 and 2015, water turbidity modeling was carried out for the Tien and Hau rivers, as well as the coastal areas in South Vietnam, the obtained mean absolute error is approximately 20%, the root means square error (*RMSE*) does not exceed 10 *NTU*. The models have a high coefficient of efficiency *ME*, approximately 90% (*ME* = 0.862), and the correlation coefficient *R* stronger than 90%. This allows for an overall assessment of the trend of changes in water flow velocity concerning the amount of sediment in the river.

## 2. RESEARCH SIGNIFICANCE

In this paper, the author used Landsat-8 multispectral satellite images with a high geometric resolution of 30-meter to analyze the turbidity of the Tien and Hau rivers. Statistical data was collected from the turbidity model based on sample points at the site to determine the amount of alluvium in the river, determining the relation between the turbidity and the erosion of the river bed and the river banks, as well as the river flow velocity imparted to the bridge substructure.

## 3. CURRENT STATE OF EROSION AND ASSESSMENT METHOD

### 3.1. State of Erosion of The Tien River

During the period from 2009 to 2013, erosion of the Tien riverbank in the section passing through Dong Thap Province continued to take place at high intensity and scale (Table 1) [11].

*Table 1. The riverbank erosion of the Tien River in the Dong Thap province in 2009-2013 [11]*

| Years | 2009 | 2010 | 2011 | 2012 | 2013 |
|---|---|---|---|---|---|
| Places eroded | 96 | 92 | 95 | 95 | 113 |
| The districts had been eroded | 34 | 35 | 39 | 36 | 32 |
| The districts can be eroded | 43 | 43 | 47 | 46 | 42 |
| Affected length (km) | 74.0 | 23.0 | 95.0 | 56.4 | 38.7 |
| Eroded area (ha) | 36.6 | 22.0 | 49.0 | 26.6 | 10.3 |

In Table 1, we can see that the erosion of the Tien riverbank in Dong Thap Province in 2009-2013 is as follows:

- Table 1 shows that from 2009 to 2013, the erosion of the Tien riverbank in Dong Thap Province exhibited the following characteristics.
- The length of the riverbank eroded or threatened with erosion ranges from 23-95 km along the entire length of the mainstream of approximately 122.9 km.
- Between 2009 and 2013, the riverbank of the Tien River lost a total of 144.42 ha of land due to riverbank erosion.

One of the main reasons for the erosion of the Tien river bank is determined by the hydrological and dynamic characteristics of the flow; geological, soil, topographical characteristics, conductor morphology, and human socio-economic activities – uncontrollable sand exploitation [11, 14].

This leads to a change in the depth of the Tien river bed. According to the statistics of the Southern Sub-Department of Inland Waterways, the depth of the Tien and Hau rivers from 2008 to the present became deeper quite fast, with an average of 3-7 m on the whole route (Figure 3).


*Figure 3. Regions of Tien and Hau rivers where the bottom of the river became deeper [12]*

In particular, in the area near the My Thuan Bridge, the riverbed depth was around 9-10 m prior to 2008, but after 2016 the depth was more than 14 m, increasing by more than 4 m, increase the effects of the water flow onto the substructure of the bridge, increasing erosion at the piers of the My Thuan bridge (Table 2).

Furthermore, the hydrological characteristics of the Mekong Delta, particularly the Tien River, are influenced by floods, rainfall, and tides, which lead to the formation of two seasons – the flood season and the dry season. Considering both the flood season and the dry season, the flow velocity of the Tien River is faster than the average velocity without erosion of the river bank (Table 2). With high flow velocity, and the ability to maintain for a relatively long time (the flood season lasts 2-3 months), the ability to erode the riverbed of the Tien river province is very high. This also leads to a significant change in the turbidity of the Tien River [12].

*Table 2. The average flow velocity and allowable average velocity without erosion of the Tien River*

| Location | Flood season | |
|---|---|---|
| | Flow velocity [m/s] | Allowable velocity [m/s] |
| Tan Chau | 2.70 | 0.58 |
| Sa Dec | 2.40 | 0.58 |
| My Thuan | 2.45 | 0.55 |
| Location | Dry season | |
| | Flow velocity [m/s] | Allowable velocity [m/s] |
| Sa Dec | 1.10 | 0.58 |
| My Thuan | 1.20 | 0.55 |

### 3.2. Documentation of Turbidity Survey Area by Satellite Image

The turbidity of the Tien and Hau rivers, as well as the estuary area, including the Saigon River, is monitored. Tien River has main estuaries flowing into the East sea such as Cung Hau, Co Chien, Ham Luong, Ba Lai, and Cua Dai. The Hau River has two main estuaries, Tranh De and Dinh An. Saigon River's main gate is Soi Rap [14].

The satellite images used for turbidity monitoring are multi-time Landsat-8 images for the period January 24, 2015, and January 24, 2014. Figure 1 shows the RGB color composite images of Landsat-8 for the period 2015 and 2014. Image 2014 is influenced by quite a lot of clouds.

Along Tien and Hau rivers, water sampling and turbidity analysis were conducted (unit: *NTU*). Water samples were taken from river cross-sections at three locations, between the river and the left and right sides of the river bank.

For the year 2015, the total number of sampling and measuring points with GPS location is 63 points. After excluding the combined raw error in the image processing, the number of points that can be used is 52 points; 45 of which are used to model turbidity, and 7 points are used as checkpoints.

For the year 2014, due to the large fraction of clouds, the total number of water sampling points at the site was 63, but in fact, only 28 water sampling points were used because clouds were obscured, near 44.44%. Out of 28 water sample points, 3 points found unreasonable points 17-T, 17-P, 18-G. Thus, the number of water sample points used for estimating the water turbidity model is 25, in which 20 points are used to build a model turbidity and 5 points are used as model checkpoints. Locations of the field sampling points are posted on the Landsat-8 image as shown in Figure 4.

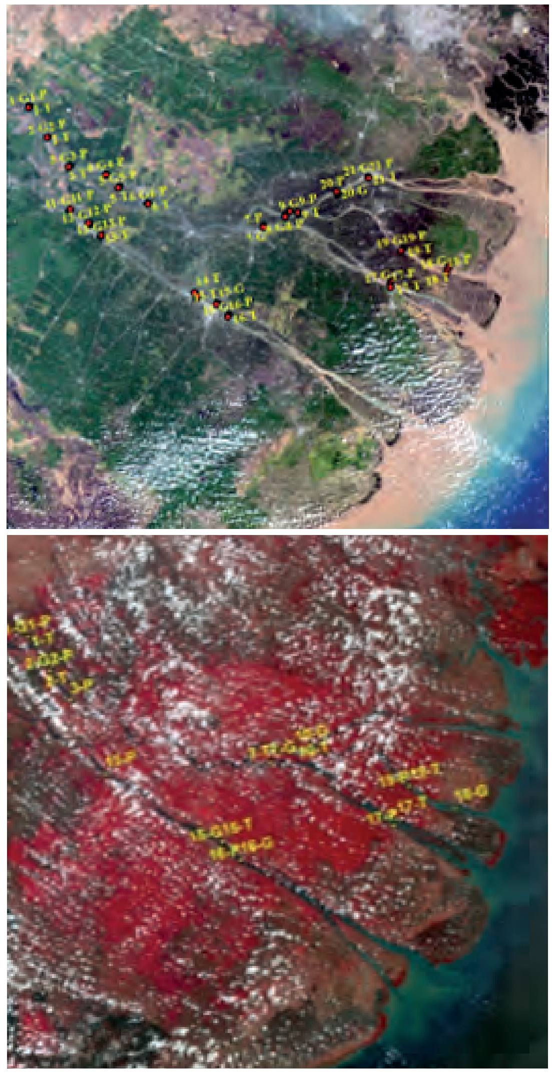

*Figure 4. Landsat-8 images from two dates 24/01/2015 (above), 24/01/2014 (down)*

### 3.3. Methodology

Figure 5 introduces $L_t$ synthesized light rays going to the receiver (sensor) from single solar rays carrying energy $E_s$, including four components: scattered rays in the atmosphere $L_p$, rays reflecting water surface $L_s$, reflected rays from the inside the waterbed $L_w$ (or the water-leaving reflection), and the bottom reflection $L_b$; means [3, 6]:

$$L_t = L_p + L_s + L_w + L_b \tag{1a}$$

Among the four components, only the $L_w$ component– the water-leaving reflection that carries information about water quality, namely turbidity (*NTU*):

$$L_w = L_t - L_s - L_p - L_b \tag{1b}$$

Depending on the depth and turbidity of the water, $L_b$ component can be zero. Equation (1b) shows that:

firstly, we need to correct the spectral radiation of the $L_t$ image due to the influence of the atmospheric environment ($L_p$). If the remote sensing reflection on the water surface is $R_{rs}$ and the remote sensing reflection below the water surface is $\rho_{rs}$, the relationship between them showed as [1, 7]:

$$R_{rs} = \frac{c \cdot R_{rs}}{(1 - k \cdot R_{rs})} \tag{2}$$

Where parameter $c$ depends on the radiation transmission coefficient in two directions from the bottom to the top of the water surface and vice versa, and also on the refractive index of the water medium. The parameter $k$ depends on the reflectivity on the water-air interface, and the ratio between the rising radiation from the water body to the radiating completely [6]. $R_{rs}$ is defined as the ratio of the radiation leaving the water surface to the receiver $L_w$ and the downward solar spectrum radiation $E_s$ (Fig. 5) [7, 8]:

$$R_{rs} = \frac{L_w}{E_s} \tag{3}$$

After correcting for the atmospheric effects on the image radiation and treating the surface reflectivity ($R_{rs}$), the bottom water reflection ($R_{rs}$) is determined from the following Equation (2).

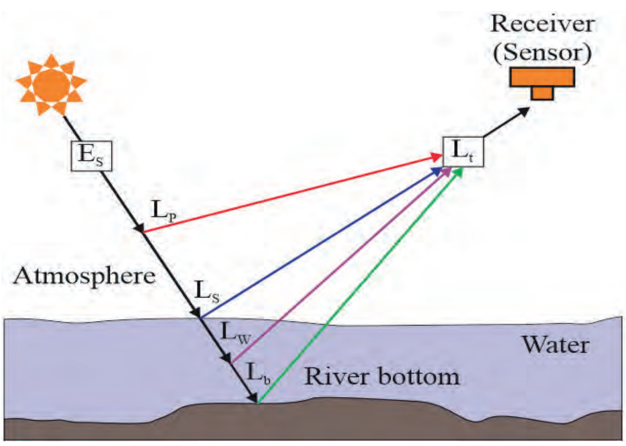


*Figure 5. Diagram of reflected ray components going to the receiver*

## 4. RESULTS AND EVALUATION

### 4.1. Set Up the Turbidity Model

Before establishing the turbidity model, it was crucial to process the satellite image radiation. The steps involved in processing satellite images are summarized below:

- Masking the land and leaves only the water surface of the Tien, and Hau River, and coastal areas.
- Adjusting image geometry and match the field sampling point grid according to the coordination on the image.
- Separating clouds and clouds shadow.
- Processing R-radiation images at the top of the atmosphere from the original DN image (quantization image)
- Processing reflective images of $\rho$ surface.
- Processing remote sensing reflection image $\rho_{rs}$.
- Creating high layer image channels from remote sensing reflection image $\rho_{rs}$ of channels R, G, B.
- Finding the relationship between the site turbidity sample and the remote sensing reflection $\rho_{rs}$ and remove the unsatisfactory image channels.
- Setting up the turbidity model.
- Calculating errors such as mean squared error, mean absolute error, etc.
- Eliminating raw errors, then reset the turbidity model and recalculate the errors.
- The process of establishing the turbidity model and calculating the error have to satisfy the following conditions:
  - An average absolute error has to be smaller than 30%, or accuracy is over 70%.
  - Correlation coefficient while building model $R^2$ is not less than 0.7.

After processing satellite image radiation and removing the raw error from site sample data, the turbidity model is built based on the relationship between remote sensing reflection of high layer image and turbidity from site samples. Then a turbidity model is selected to meet upper requirements. Figure 6 shows the turbidity model selected based on 45 field sample points for the period 2015 which is the linear equation: $y = 1.1542x - 3.247$ (4) with strong correlation coefficient $R^2 = 0.8617$ ($R = 92.84\%$). The turbidity model based on 20 points for the period 2014 is an exponential Equation (5), with a strong correlation coefficient $R^2 = 0.9048$ ($R = 95.12\%$) (Figure 6).

- Model of turbidity period 2015 has a form:

$$\begin{gathered} DODUC(NTU) = 1.1542 \cdot x - 3.247 \\ x = 173.16 \cdot b_{ü} + 53.65 \cdot b \ + 55.65 \cdot b \ - 211.95 \end{gathered} \tag{4}$$

where: $b_1$, $b_2$, $b_3$ are high-layer images generated from remote sensing reflection $\rho_{rs}$ of RBG channels.

- Model of turbidity period 2014 has a form:

$$\begin{gathered} DODUC(NTU) = 5.648 \cdot e^{x} \\ x = 5.818 \cdot b_1 + 1.803 \cdot b_2 + 1.870 \cdot b_3 - 7.122 \end{gathered} \tag{5}$$

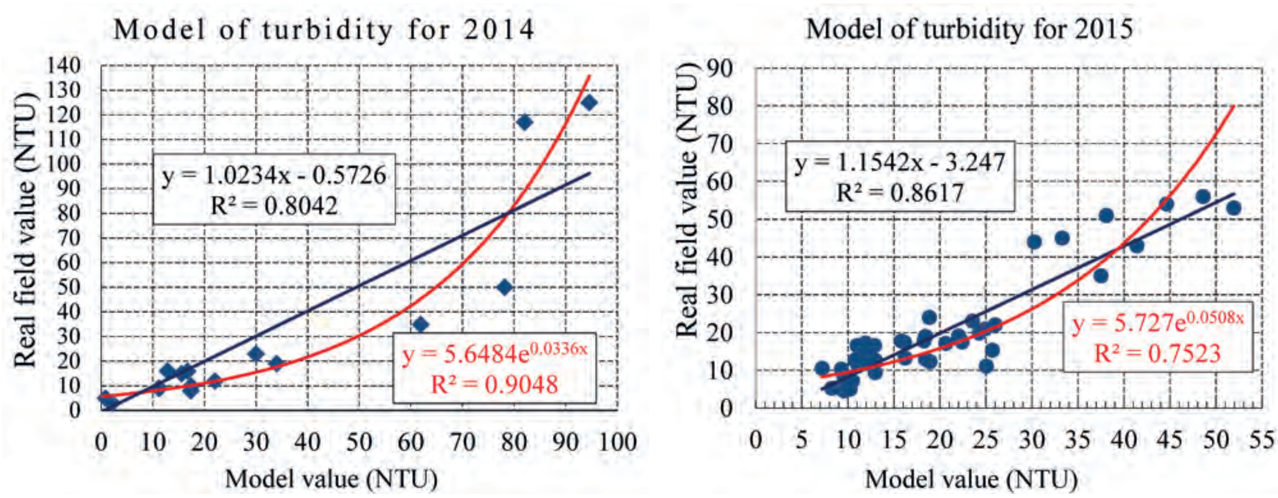


*Figure 6. Turbidity model for 2014 and 2015*

where: $b_1$, $b_2$, $b_3$ are high-layer images generated from remote sensing reflection $\rho_{rs}$ of RBG channels.

The next important step is to evaluate the reliability and accuracy of the two models Equation (4) and Equation (5) presented in sections 4.2 and 4.3. Therefore, other statistical parameters were used to assess model performance. In this paper (Table 3), useful statistical parameters are as follows:

- Correlation coefficients, $R^2$:

$$R^2 = \left[ \frac{\sum_{i=1}^{n} (x_i - \bar{x}_i)(y_i - \bar{y}_i)}{\sqrt{\sum_{i=1}^{n} (x_i - \bar{x}_i)^2} \sqrt{\sum_{i=1}^{n} (y_i - \bar{y}_i)^2}} \right]^2 \tag{6}$$

- Root mean square error, *RMSE*:

$$RMSE = \sqrt{\frac{1}{n} \sum_{i=1}^{n} (x_i - y_i)^2} \tag{7}$$

- Mean absolute error, *MAE*:

$$MAE = \frac{1}{n} \left[ \sum_{i=1}^{n} (x_i - y_i)^2 \right]$$
$$MAE \text{ in } \% = \frac{MAE}{\bar{x}_i} \cdot 100 \tag{8}$$

- Coefficient of modeling efficiency, *ME*:

$$ME = 1 - \left[ \frac{\sum_{i=1}^{n} (x_i - y_i)^2}{\sum_{i=1}^{n} (x_i - \bar{x}_i)^2} \right] \tag{9}$$

where: $x_i$ are the observed values with the mean of; $y_i$ are the modeled values with the mean of; $n$ is the number of observations; $i = 1, 2, 3, ..., n$.

### 4.2. Evaluate a Turbidity Model Based on Field Sample Points

The results of the evaluation of the turbidity model on 45 sample points for 2015 and 20 sample points for

*Table 3. The parameters to evaluate the turbidity model on the constructed model points for 2 periods*

| For 2014 | | For 2015 | |
|---|---|---|---|
| **Parameters** | **Real value** | **Parameters** | **Real value** |
| Mean square error | 9.987(*NTU*) | Mean square error | 5.267(*NTU*) |
| Average absolute error | 5.778(*NTU*) ≡ 23.63% | Average absolute error | 4.186(*NTU*) ≡ 21.29% |
| Correlation coefficient *R* ($R^2$) | 0.958 ($R^2$ = 0.9048) | Correlation coefficient *R* ($R^2$) | 0.928 ($R^2$ = 0.8617) |
| Linear regression coefficient *α* | 1.0234 | Linear regression coefficient *α* | 1.154 |
| Linear regression deviation *β* | 0.573 | Linear regression deviation *β* | 3.247 |
| Minimize the field turbidity | 3.0(*NTU*), point 2T | Minimize the field turbidity | 4.5(*NTU*), point 2G |
| Number of model points | 20 | Number of model points | 45 |
| Efficiency coefficients model *ME* | 0.914 | Efficiency coefficients model *ME* | 0.862 |

2014 are summarized in Table 3. Both turbidity models for 2015 and 2014 both have a high ME coefficient, nearly 1, with a difference of only 5%. In 2015 the model uses twice more points than 2014, giving a small mean square error approximately half that of 2014, and an average absolute error of 1.11 times less.

### 4.3. Evaluate the Model on The Checkpoints

#### 4.3.1. Evaluation by mean square error and average absolute error

After setting up a model with 7 points for 2015 and 5 points for 2014 (Table 4) called checkpoints were used to evaluate the model. The mean square error and average absolute error were calculated based on the difference in *NTU* values from the model and the field sample points as shown in Tables 4 and 5. The average absolute error for 2015 was 20.54%; for 2014 was 22.50%, both less than 30%.

#### 4.3.2. Evaluation by regression function

The turbidity model was evaluated using checkpoints based on the regression function shown in Figure 7. The correlation coefficient of the regression function for 2015 and 2014 is quite strong with $R^2$ = 0.8829 ($R$ = 93.96%) and $R^2$ = 0.8920 ($R$ = 94.44%). The coefficient of the regression line angle of both periods compared to the ideal value is about ±17% difference, ($\alpha$ = 0.823 and $\alpha$ = 1.174). Table 6 summarized the results of the turbidity model assessment based on the checkpoints for 2015 and 2014. The statistical parameters in Table 5 for the 2 periods are not significantly different. It should be noted that the mean square error and the mean absolute error of the two periods are both smaller than the field minimum values.

The turbidity of the Tien river and Hau river in Southern Vietnam based on the turbidity model by functions (4) and (5) for 2015, 2014 is shown in Figure 8. Additionally, the distribution of turbidity maps for the Tien River, Hau River, and estuary coast in Southern Vietnam is shown in Figure 9.

*Table 4. Evaluate the turbidity model accuracy at the sample points*

| For 2014 | | | | | For 2015 | | | | |
|---|---|---|---|---|---|---|---|---|---|
| No. | Point | Turbidity from field samples ($NTU_{TĐ}$) | Turbidity from the model ($NTU_A$) | Absolute error | No. | Point | Turbidity from field samples ($NTU_{TĐ}$) | Turbidity from the model ($NTU_A$) | Absolute error |
| 1. | 1-T | 5 | 5.15864 | 0.15864 | 1. | 2-T | 10.4 | 6.7946 | 3.6054 |
| 2. | 13-P | 9 | 5.75 | 3.25 | 2. | 5-G | 8.5 | 14.5287 | 6.0287 |
| 3. | 15-P | 20 | 11.5061 | 8.4939 | 3. | 12-T | 12.6 | 13.0733 | 0.4733 |
| 4. | 17-T | 30 | 25.1651 | 4.8349 | 4. | 9-P | 35 | 25.8761 | 9.1239 |
| 5. | 16-P | 11 | 10.8576 | 0.1424 | 5. | 15-P | 25 | 27.8328 | 2.8328 |
| | | | | | 6. | 18-G | 49 | 61.8167 | 12.8168 |
| | | | | | 7. | 17-G | 43 | 57.0483 | 14.0483 |
| Average value | | 15 | 11.6874 | 3.3759 | Average value | | 26.214 | 29.5672 | 3.3532 |
| Mean square error | | | | 4.6072 | Mean square error | | | | 8.4723 |
| Average absolute error | | | | 22.50% | Average absolute error | | | | 20.54% |

*Table 5. The parameters evaluate the turbidity model at the checkpoints for 2 periods*

| For 2014 | | For 2015 | |
|---|---|---|---|
| **Parameters** | **Real value** | **Parameters** | **Real value** |
| Mean square error | 4.607(*NTU*) | Mean square error | 8.472(*NTU*) |
| Average absolute error | 3.376(*NTU*) ≡ 22.50% | Average absolute error | 6.,990(*NTU*) ≡ 20.54% |
| Correlation coefficient $R$ ($R^2$) | 0.944 (0.892) | Correlation coefficient $R$ ($R^2$) | 0.940 (0.883) |
| Linear regression coefficient $\alpha$ | 1.174 | Linear regression coefficient $\alpha$ | 0.823 |
| Linear regression deviation $\beta$ | 1.281 | Linear regression deviation $\beta$ | 2.817 |
| Minimize the field turbidity | 5.0(*NTU*), point 1T | Minimize the field turbidity | 8.5(*NTU*), point 5G |
| Number of model points | 5 | Number of model points | 7 |

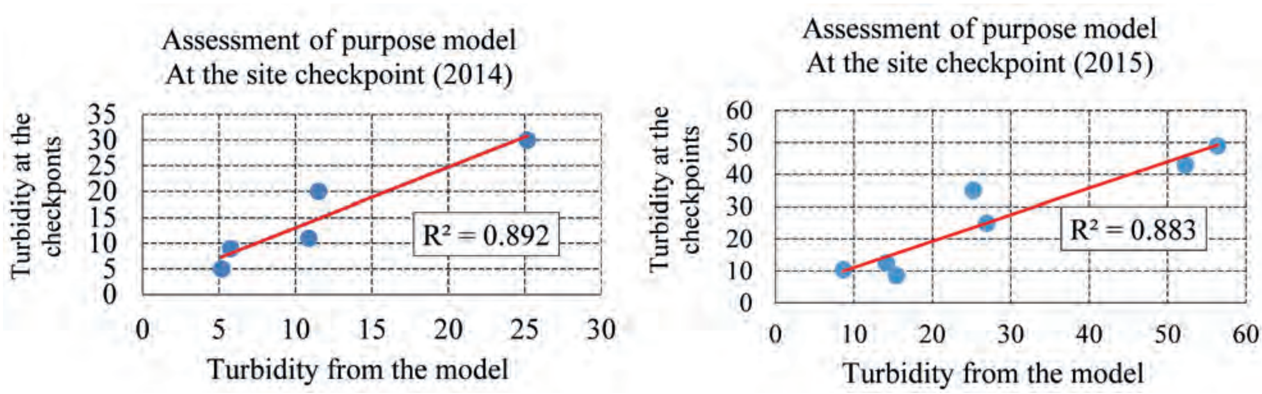


*Figure 7. Evaluation of the turbidity model at the checkpoints based on the regression function for 2015 and 2014*

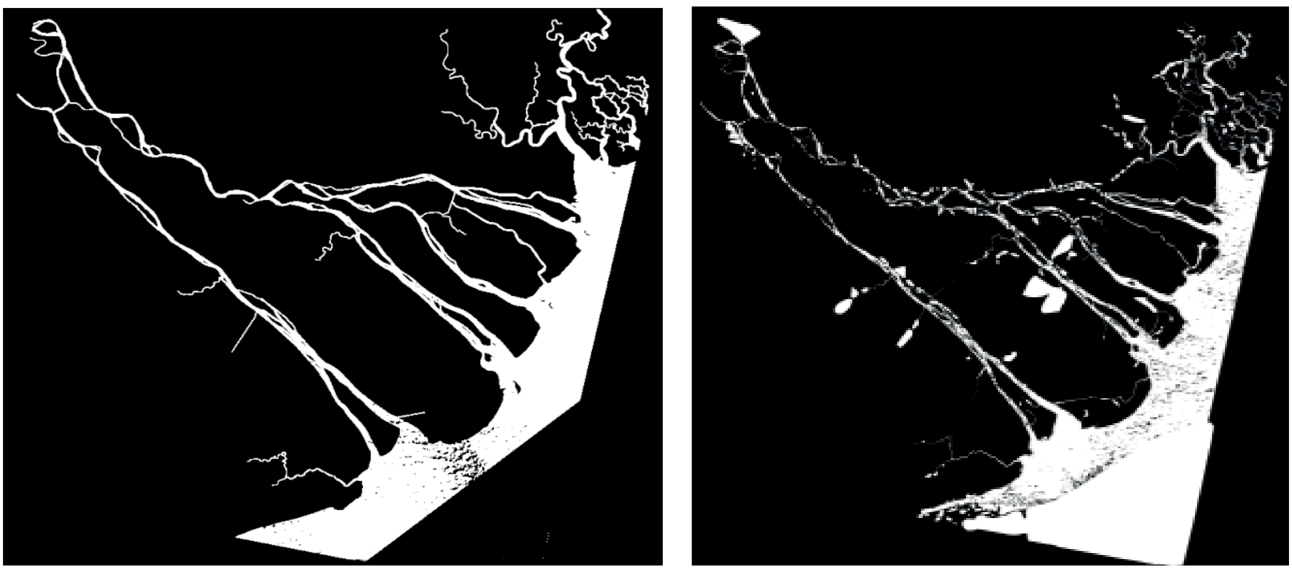

*Figure 8. Digital image of turbidity in Tien and Hau rivers for 2015 (left) for 2014 (right)*

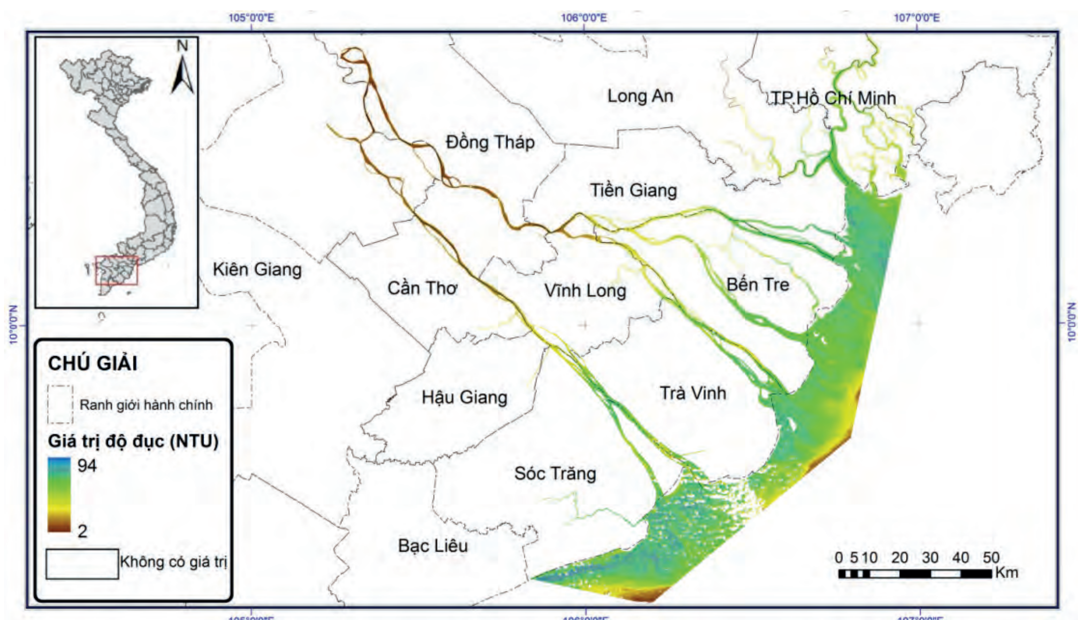


*Figure 9. Turbidity distribution map of Tien, Hau river, and coastal estuary (January 24, 2015)*

#### 4.3.3. Discussion

Based on the calculation results, some general comments are as follows:

– The mean square error for determining the turbidity is less than 10 *NTU*.
– The accuracy of determination of turbidity reaches 80%.
– The strong correlation coefficient *R*, over 90%. The efficiency coefficient of the *ME* model is approximately 90%.
– Linear regression coefficient $\alpha$ is less than 20% different from the ideal value.
– The linear regression deviation $\beta$ is all smaller than the field turbidity minimum value (less than 5 *NTU*).
– The above results show that: turbidity model for 2015 and 2014 determined by equations (4) and (5) is reliable, consistent with the objective reality between the results extracted from remote sensing and field sample data.
– The results of the treatment of turbidity classification from the digital image of turbidity (Figure 8) on ArcGIS (Figure 9) showed that: turbidity concentration in Tien and Hau rivers increases when entering the territory of Ben Tre, Tra Vinh, and Soc Trang provinces. Turbidity concentrates in the coastal areas and decreases when offshore from 94 (*NTU*) to 2 (*NTU*) over a distance of 20 km.

## 5. CONCLUSION

Turbidity is considered an important indicator in assessing the level of silt (sand) in the river, allowing sediment alluvial to build up river banks, monitoring the degree of water corrosion in the bridge structure to build an effective maintenance and conservation program for the bridge in response to climate change.

The use of satellite images to monitor surface water turbidity in particular and the environment, in general, is a great idea in the application of high technology to promote economic development, as well as planning and management resources (water and sand), exploitation, and operation of bridges in the river corridor, minimizing adverse impacts of the water flow on the bridge, is the general trend in the world.

Using satellite remote sensing technology allows monitoring the spatial distribution of water quality, particularly turbidity on the square grid with the resolution equal to the geometrical resolution of the multi-spectral image with low-cost for water metering and sampling at the site. The results using Landsat-8 satellite images allow determining the turbidity in the square grid 30 × 30 m with the accuracy of approximately 80% of Tien River, Hau River, and the coastal area.

With a small number of water sample points (63 points) at the site for both rivers in the Delta Mekong from upstream to near the coastal estuary, a turbidity model was built, and allow to determine turbidity for any point at the time of satellite scanning with a median error less than 10 *NTU*.

For further improved accuracy, requires uniformity between site work (water sampling) at the time the satellite makes the image, and at the same time overcome cloud cover.

The changes of the turbidity in the Tien and Hau river bed, show the erosion situation to identify causes as a scientific basis to propose solutions to stabilize river banks, ensure structural diagrams of bridges (My Thuan Bridge), respond to climate change, and minimizing the impact damage to the bridge is essential.

## REFERENCES

[1] Gordon H.R., Brown O.B., Evans R.H., Brown J.W., Smith R.C., Baker K.S., Clark D.K., *A semi-analytic radiance model of ocean color.* J. Geophys. Res., Vol. 93, 1988, pp.10909-10924.
[2] Keiser M., Aboulela H., et. al., *Spectral enhancement of the SPOT imagery data to assess marine pollution near Port Said*, Egypt. PIERS Proceedings, July 2-6, 2008, Cambridge, USA.
[3] Lee Z.P., Carder K.L., Hawes S.K., Steward R.G., Peacock T.G., Davis C.O., *Model for the interpretation of hyperspectral remote sensing reflectance*. Applied Optics, vol. 33, 1994, pp. 5721-5732.
[4] Liew S.C., Saengtuksin B., Kwoh L.K., 2011, *Mapping Water Quality of Coastal and Inland Waters Using High-Resolution Worldview-2 Satellite Imagery*. Proc. 34th. International Symposium on Remote Sensing of Environment, 10-15 April 2011, Sydney, Australia.
[5] Manchino G., Nole A., et al., *Assessing water quality by remote sensing in a small lake: the case study of Monticchio lakes in Southern Italy*. Biosciences and Forestry, 2009, pp. 154-164.
[6] Mobley C.D., *Light and Water: Radiative Transfer in Natural Water*, Academic, New York, 1994.
[7] Mobley C.D., *Estimation of the remote-sensing reflectance from above-surface measurements*. Applied Optics, Volume 38, 1999, pp. 7442-7455.
[8] Morel A., Gentili B., *Diffuse reflectance of oceanic waters: II. The implication of bi-directionality for the remote-sensing problem*, Applied Optics, Vol. 35, 1996, pp. 4850-4861.

[9] Yuan-Fong Su, Jun-Jih Liou, Ju-Chen Hou, Wei-Chun Hung, Shu-Mei Hsu, Yi-Ting Lien, Ming-Daw Su, Ke-Sheng Cheng, Yeng-Fung Wang, 2008. *A multivariate model for coastal water quality mapping using satellite remote sensing images*. Sensors, Vol. 8, 2008, pp. 6321-6339.

[10] Luong Chinh Ke, Ho Thi Van Trang, Vu Huu Liem, Tran Ngoc Tuong, Pham Thi Duyen., *Assessment of surface water pollutant models of estuaries and coastal zone of Quang Ninh – Hai Phong using Spot-5 images*. Polish Academy of Sciences, Geodesy and Cartography. Vol. 64, No 1, 2015, pp. 29-42.

[11] *Dong Thap Department of Agriculture and Rural Development*, Report of the prevention, fighting, and overcoming of riverbank erosion in 2009, 2010, 2011, 2012, 2013, Dong Thap, Vietnam 2013.

[12] Trinh Phi Hoang., *Study of the main weather disturbances causing rain-flooding in the Mekong Delta River*. Science Journal of Pedagogical University Ho Chi Minh City, 43 (81), 2013, pp. 107-116.

[13] *Report of My Thuan cable-stayed bridge – Test results*. Fressinet Vietnam, 2016.

[14] Duong Thi Truc. *The water surface quality of Tien river in the area of Tan Chau district*, An Giang province. Can Tho University Journal of Science, Vol. 55, Issue: Environment and Climate Change (2), 2019, pp. 53-60.

[15] Riki Mukhaiyar. *Digital image and remote sensing image as data for identification of a quality of a non-point source pollutant in Ciliwung river*, Indonesia. International Journal of GEOMATE, Vol. 12, Issue 32, April 2017, pp. 142-151.